

See discussions, stats, and author profiles for this publication at: <https://www.researchgate.net/publication/270826741>

# Effect of Low Viscous Nondipolar Solvent on the Rotational Diffusion of Structurally Similar Nondipolar Solutes in an Ionic Liquid

ARTICLE *in* THE JOURNAL OF PHYSICAL CHEMISTRY B · JANUARY 2015

Impact Factor: 3.3 · DOI: 10.1021/jp512456c · Source: PubMed

---

CITATIONS

3

---

READS

17

2 AUTHORS, INCLUDING:



Sugosh Prabhu

Bhabha Atomic Research Centre

10 PUBLICATIONS 22 CITATIONS

SEE PROFILE

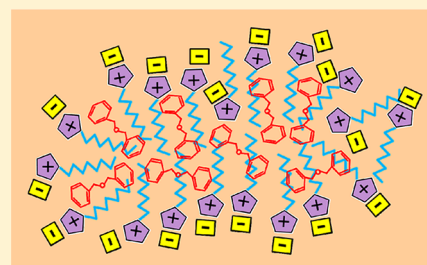
# Effect of Low Viscous Nondipolar Solvent on the Rotational Diffusion of Structurally Similar Nondipolar Solutes in an Ionic Liquid

Sugosh R. Prabhu and G. B. Dutt\*

Radiation and Photochemistry Division, Bhabha Atomic Research Centre, Trombay, Mumbai 400 085, India

## S Supporting Information

**ABSTRACT:** Fluorescence anisotropies of two structurally similar nondipolar solutes, 2,5-dimethyl-1,4-dioxo-3,6-diphenylpyrrolo[3,4-*c*]pyrrole (DMDPP) and 1,4-dioxo-3,6-diphenylpyrrolo[3,4-*c*]pyrrole (DPP), have been measured in 1-methyl-3-octylimidazolium hexafluorophosphate–dibenzyl ether ([MOIM][PF<sub>6</sub>])–DBE mixtures to understand how the addition of a low viscous nondipolar solvent influences solute rotation. The data when analyzed with Stokes–Einstein–Debye hydrodynamic theory reveals that the measured reorientation times of DMDPP are closer to the predictions of slip boundary condition, whereas those of DPP follow stick hydrodynamics. This outcome arises due to specific interactions between DPP and the solvent medium. Nevertheless, the important result of this study is that the rotational diffusion of DMDPP becomes gradually slower with an increase in the mole fraction of DBE ( $x_{\text{DBE}}$ ) for a given viscosity and temperature. In contrast, such a trend is not noticed for the hydrogen-bond donating solute DPP. Instead, two sets of reorientation times have been obtained, one corresponding to  $x_{\text{DBE}} = 0.0$ –0.2 and the other  $x_{\text{DBE}} = 0.4$ –1.0. The results for DMDPP have been rationalized on the basis of the organized structure of [MOIM][PF<sub>6</sub>], which attains homogeneity at the microscopic level with an increase in  $x_{\text{DBE}}$ . In case of DPP, however, the propensity of the solute to be in the neighborhood of DBE, as a consequence of its stronger hydrogen bond accepting ability compared to the ionic liquid, appears to be the reason for the observed behavior.



## 1. INTRODUCTION

In recent times, numerous studies have been carried out with ionic liquids in the presence of additives.<sup>1–11</sup> The results of these investigations in effect have enabled us to understand how the structure and subsequently the dynamics of solutes dissolved in the binary systems are altered compared to neat ionic liquids. It has been well-established that due to the presence of Coulombic, hydrogen bonding, and van der Waals interactions, ionic liquids form organized structures with the segregation of nonpolar and ionic regions.<sup>12</sup> Addition of an organic solvent usually induces changes in the organized structure of the ionic liquids, which in turn has an effect on the dynamical processes such as solute rotation and solvation dynamics. However, rotational diffusion studies involving structurally similar nonpolar (9-phenylanthracene, 9-PA) and charged (rhodamine 110, R110) solutes in propylammonium nitrate–propylene glycol (PAN–PG) mixtures suggest that the reorientation times ( $\tau_r$ ) of the two solutes scale linearly with viscosity ( $\eta$ ) at a given temperature ( $T$ ) and the rotational diffusion of each solute is similar in PAN, PG, and PAN–PG mixtures.<sup>8</sup> This observation has been rationalized on the basis of the disordered lamellar structure present in PAN, which does not provide compact organized domains so that solute rotation is affected as in the case of ionic liquids having longer alkyl chains. Recent small-angle neutron-scattering studies carried out with protic ionic liquids–alcohol mixtures indicate that although short-chain alcohols disrupt the inherent nanostructure of these ionic liquids, they do not generate a qualitatively different solution

structure.<sup>10</sup> In contrast to PAN–PG mixtures, rotational diffusion measurements dealing with 9-PA and R110 in 1-methyl-3-octylimidazolium tetrafluoroborate–diethylene glycol ([MOIM][BF<sub>4</sub>])–DEG mixtures reveal an apparent influence of the organized structure of the ionic liquid on solute rotation. Nevertheless, with an increase in the mole fraction of DEG, it has been observed that [MOIM][BF<sub>4</sub>])–DEG mixtures attain homogeneity at the microscopic level.<sup>9</sup>

Rotational diffusion studies carried out in neat ionic liquids essentially provide information pertinent to solute–ionic liquid interactions, microenvironment experienced by the solute molecules, and other nonhydrodynamic effects. As a consequence, a good number of articles dealing with this topic have appeared in literature recently.<sup>13–37</sup> By extending these investigations in ionic liquid–organic solvent binary mixtures, the complex nature of the mixtures can be unraveled at the molecular level. It may be noted that a majority of the studies involving binary mixtures have employed organic solvents that are either polar or possess hydroxyl functional groups and such solvents are most likely to be solubilized in the ionic region of the ionic liquids. In other words, polar solvents interact with the charged components of the ionic liquids and disrupt the organized structure. In view of the existing scenario, it would be prudent to find out what happens if a nondipolar solvent is

Received: December 15, 2014

Revised: January 12, 2015

Published: January 12, 2015



added to the ionic liquid. Will it be located in the nonpolar domains of the ionic liquid? What will be its effect on the organized structure of the ionic liquid? How will the dynamics of the solute molecules be influenced? To address these issues, the present study has been undertaken wherein the effect of a low viscous nondipolar solvent on the rotational diffusion of structurally similar nondipolar solutes dissolved in an ionic liquid will be explored. For this purpose, we have measured temperature-dependent fluorescence anisotropies of nondipolar solutes, 2,5-dimethyl-1,4-dioxo-3,6-diphenylpyrrolo[3,4-*c*]-pyrrole (DMDPP) and 1,4-dioxo-3,6-diphenylpyrrolo[3,4-*c*]-pyrrole (DPP), in 1-methyl-3-octylimidazolium hexafluorophosphate ([MOIM][PF<sub>6</sub>]), dibenzyl ether (DBE), and also in ionic liquid–organic solvent mixtures at different mole fractions of DBE ( $x_{\text{DBE}}$ ). Figure 1 gives the molecular structures of DMDPP

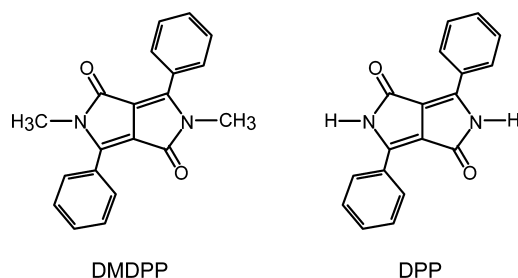


Figure 1. Molecular structures of the solutes.

and DPP. The rotational diffusion of these solutes has been investigated in ionic liquids<sup>16,17</sup> and organic solvents.<sup>38–46</sup> It has been noticed that the reorientation times of DPP are significantly longer compared to DMDPP due to the ability of the former to experience specific interactions with the solvent medium via the two NH groups. We hope that the outcome of this work will shed light on the location of the solutes in [MOIM][PF<sub>6</sub>]-DBE mixtures, their interactions with the surroundings, and also the influence of DBE on the organized structure of the ionic liquid.

## 2. EXPERIMENTAL SECTION

The ionic liquid [MOIM][PF<sub>6</sub>] and spectroscopy grade DBE were purchased from io-li-tec, Germany and Sisco Research Laboratories Pvt. Ltd., India, respectively. The solutes DMDPP and DPP were obtained from Ciba Specialty Chemicals, Inc., Switzerland. The stated purity of [MOIM][PF<sub>6</sub>] is >99% with <100 ppm water content and <100 ppm halide ion concentration. Water content of the ionic liquid and the organic solvent was estimated by Karl Fischer titration with the aid of a Metrohm 831 KF Coulometer and found to be <100 ppm. The samples with desired mole fractions of DBE in [MOIM][PF<sub>6</sub>] were prepared by weighing and mixing appropriate amounts of the two liquids in glass bottles. Both [MOIM][PF<sub>6</sub>] and DBE are easily miscible upon gentle sonication.

Absorption and fluorescence spectra of the samples were recorded using a Jasco V-650 spectrophotometer and a Hitachi F-4500 spectrofluorometer, respectively. The absorbance of the samples was maintained in the range of 0.1–0.15 at the wavelength of excitation. Fluorescence anisotropy decays were measured using a time-correlated single-photon counting spectrometer that was purchased from Horiba Jobin Yvon, U.K. The instrumental details and the description concerning the measurement of anisotropy decays have been discussed in our earlier publication.<sup>26</sup> The samples containing the probes

DMDPP and DPP were excited at 451 nm, and the emission was monitored around 550 nm. The anisotropy decay measurements of DMDPP and DPP were carried out over the temperature range 298–348 K in neat ionic liquid,  $x_{\text{DBE}} = 0.2$  and 0.4. However, in case of samples involving  $x_{\text{DBE}} = 0.6–1.0$ , the measurements were performed from 278 to 348 K or until the value of  $\tau_r$  is about 300 ps. Each measurement was repeated 2–3 times, and the average values are reported. Reorientation times were obtained from the analysis of anisotropy decays with the aid of the software supplied by Horiba Scientific. Viscosities of [MOIM][PF<sub>6</sub>], DBE, and [MOIM][PF<sub>6</sub>]-DBE mixtures were measured as a function of temperature using a Physica MCR 101 rheometer, and the uncertainties on the measured numbers are about 5%.

## 3. RESULTS AND DISCUSSION

The viscosities of neat DBE and [MOIM][PF<sub>6</sub>] are 4.96 and 701 mPa s, respectively, at 298 K. These numbers suggest that the viscosity of the organic solvent is significantly lower compared to that of the ionic liquid. The variation of the viscosity of the ionic liquid with  $x_{\text{DBE}}$  over the temperature range of 298–348 K is displayed in Figure 2. The nonideal nature of

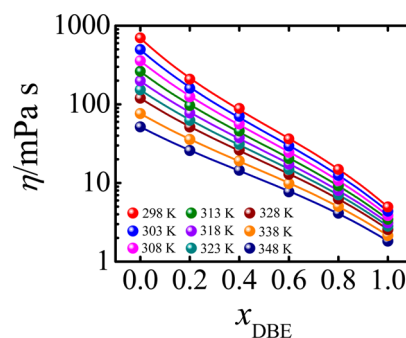


Figure 2. Plots of viscosities of [MOIM][PF<sub>6</sub>]-DBE mixtures as a function of  $x_{\text{DBE}}$  at different temperatures; the curves passing through the data points represent the trends in the variation.

[MOIM][PF<sub>6</sub>]-DBE mixtures can be assessed by calculating the parameter, excess viscosity ( $\eta^E$ ), with the aid of the following equation:

$$\eta^E = \eta - [x_{\text{DBE}}\eta_{\text{DBE}} + (1 - x_{\text{DBE}})\eta_{[\text{MOIM}][\text{PF}_6]}] \quad (1)$$

In eq 1, the parameters  $\eta$ ,  $\eta_{\text{DBE}}$ , and  $\eta_{[\text{MOIM}][\text{PF}_6]}$  represent the viscosities of the solvent mixture, the organic solvent, and the ionic liquid, respectively. Figure 3 gives plots of  $\eta^E$  versus  $x_{\text{DBE}}$  at different temperatures. It is evident from the figure that [MOIM][PF<sub>6</sub>]-DBE mixtures exhibit negative excess viscosity at all temperatures with minima centered around  $x_{\text{DBE}} = 0.3$  and upon increasing the temperature,  $\eta^E$  becomes less negative. These large negative numbers indicate the loss of electrostatic interactions in ionic liquid–organic solvent mixtures compared to neat ionic liquid, and such a behavior has also been noticed in case of numerous ionic liquid–organic solvent mixtures.<sup>8,9,47–51</sup> In view of the nonideal behavior exhibited by these liquid mixtures, it would be interesting to find out the influence of DBE on the rotational diffusion of DMDPP and DPP in [MOIM][PF<sub>6</sub>].

Emission spectra of DMDPP and DPP in DBE, [MOIM][PF<sub>6</sub>], and [MOIM][PF<sub>6</sub>]-DBE mixtures are displayed in Figure 4. It can be noticed from the figure that with an increase in  $x_{\text{DBE}}$  from 0.0 to 1.0, emission spectra of both the solutes are

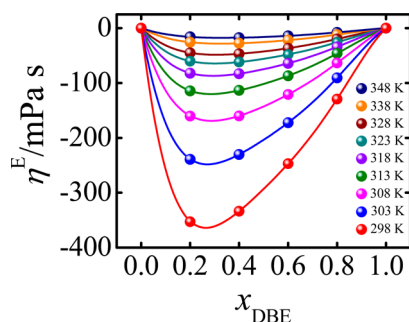


**Figure 3.** Plots of excess viscosities of [MOIM][PF<sub>6</sub>]-DBE mixtures vs mole fraction of DBE from 298 to 348 K. The curves passing through the data points represent the variation of  $\eta^E$  with  $x_{\text{DBE}}$ , and these curves are obtained by fitting the data to fifth-order polynomial functions.

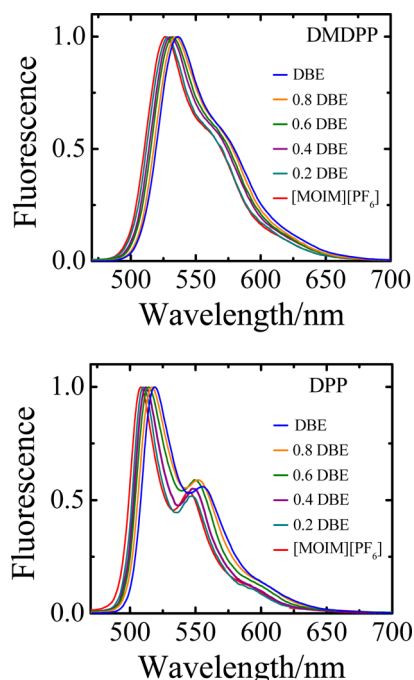


**Figure 4.** Normalized emission spectra of DMDPP and DPP in DBE, [MOIM][PF<sub>6</sub>], and [MOIM][PF<sub>6</sub>]-DBE mixtures. These spectra were recorded by exciting the solutes at 451 nm.

red-shifted by about 10 nm. Nevertheless, it is difficult to comprehend the changes in the nature of the microenvironment experienced by the solute molecules with an increase in  $x_{\text{DBE}}$  from these small spectral shifts. To get a better appreciation of the nature of the interactions experienced by DMDPP and DPP in [MOIM][PF<sub>6</sub>]-DBE mixtures, reorientation times of the solute molecules have been considered. The reorientation times of DMDPP and DPP have been obtained from the analysis of anisotropy decay curves, and single-exponential function is adequate to fit these decay curves for the systems employed in this work. The reorientation times obtained in this manner for both the solutes along with the viscosities of the neat liquids and the solvent mixtures are given in the Supporting Information. The uncertainties on the  $\tau_r$  values are in the range of 5–10%. To comprehend the rotational diffusion of DMDPP and DPP in neat liquid, DBE, and [MOIM][PF<sub>6</sub>]-DBE mixtures, Stokes–Einstein–Debye (SED) hydrodynamic theory has been considered.<sup>52,53</sup> According to this theory, the reorientation time of a solute molecule is given by eq 2.

$$\tau_r = \frac{\eta V_h}{kT} \quad (2)$$

In the above equation,  $k$  and  $V_h$  are the Boltzmann constant and hydrodynamic volume of the solute, respectively. Hydrodynamic volume is the volume experienced by the solute molecule in the solvent medium, which is a product of van der Waals volume ( $V$ ), shape factor ( $f$ ), and the boundary condition parameter ( $C$ ). The parameters,  $V$  and  $f$  account for the size and shape of the solute, while  $C$  determines the extent of coupling between the solute and the solvent.<sup>54–56</sup> Even though  $C$  is a measure of solute–solvent frictional coupling, the SED theory takes into consideration only the size of the solute molecule while calculating the boundary condition parameter. Despite this shortcoming, the SED theory is reasonably successful in describing the rotational diffusion of medium-sized solute molecules in different kinds of solvents. The two limiting values for  $C$  are the hydrodynamic slip ( $C_{\text{slip}}$ ), which satisfies the inequality  $0 < C_{\text{slip}} \leq 1$ , and hydrodynamic stick with  $C = 1$ . To apply the SED theory for the systems under investigation, the solutes have been treated as asymmetric ellipsoids as their dimensions along the three principal axes of rotation are different. The axial radii of DMDPP and DPP are identical ( $8.2 \times 4.3 \times 1.9 \text{ \AA}^3$ ), whereas the volumes of the former and latter are 281 and  $246 \text{ \AA}^3$ , respectively. Since the dimensions of the two solutes are identical, their shape factors and solute–solvent coupling parameters with slip boundary condition are also the same ( $f = 2.03$  and  $C_{\text{slip}} = 0.32$ ). Nevertheless, the calculated reorientation times of the two solutes differ by 14% as a result of the higher van der Waals volume of DMDPP by the same magnitude. The details of the calculation are described in our earlier publication.<sup>38</sup> To find out how well the SED theory rationalizes the observed results, anisotropy decays of DMDPP and DPP in  $x_{\text{DBE}} = 0.2$  and  $0.8$  measured at identical  $\eta/T$  are displayed in Figure 5. It can be noticed from the figure that the

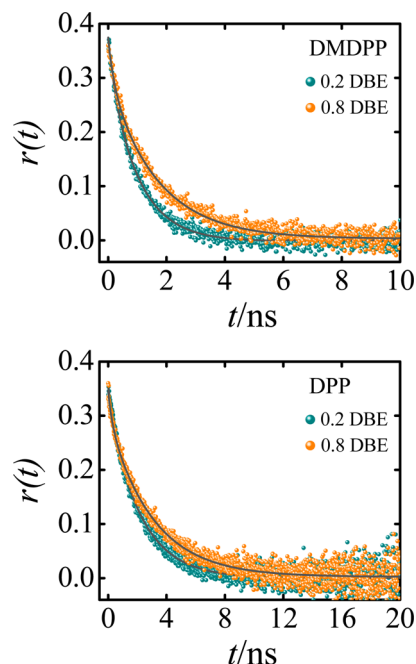


**Figure 5.** Anisotropy decays of DMDPP and DPP in [MOIM][PF<sub>6</sub>]-DBE mixtures along with the fitted curves. The temperatures have been chosen such that  $\eta/T$  value for the two mixtures is identical, which is  $0.074 \text{ mPa s K}^{-1}$ .



anisotropy decays for both the solutes are slower at  $x_{\text{DBE}} = 0.8$  and the difference is more pronounced in case of DMDPP compared to DPP. In other words, it is evident from these plots that the rotation of the solutes becomes slower with an increase in  $x_{\text{DBE}}$ , which cannot be rationalized by the SED theory.

To get a better appreciation of the rotational diffusion of DMDPP in [MOIM][PF<sub>6</sub>]-DBE mixtures,  $\tau_r$  versus  $\eta/T$  plots are presented in Figure 6, and a careful inspection of these plots

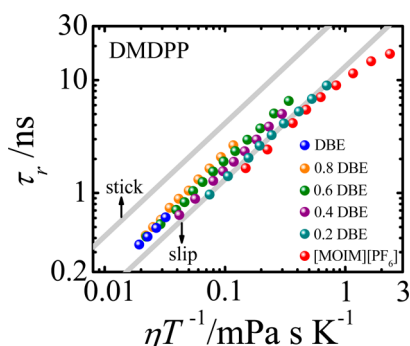


**Figure 6.** Plots of  $\tau_r$  vs  $\eta/T$  for DMDPP in [MOIM][PF<sub>6</sub>]-DBE mixtures. The SED slip and stick lines are also shown in the figure.

reveals the following features. The reorientation times of DMDPP are closer to the predictions of slip hydrodynamics and become progressively slower with an increase in  $x_{\text{DBE}}$  at a given  $\eta/T$ . Linear least-squares fits of the data resulted in the following relationships between  $\tau_r$  and  $\eta/T$ , where  $N$  and  $R$  represent the number of data points and regression coefficient, respectively.

$$x_{\text{DBE}} = 0.0 \quad \tau_r = (9.60 \pm 0.04)(\eta/T)^{0.87 \pm 0.04} \quad (N = 9, R = 0.9928)$$

$$x_{\text{DBE}} = 0.2 \quad \tau_r = (12.9 \pm 0.2)(\eta/T)^{0.99 \pm 0.01} \quad (N = 9, R = 0.9997)$$

$$x_{\text{DBE}} = 0.4 \quad \tau_r = (17.5 \pm 0.2)(\eta/T)^{1.04 \pm 0.01} \quad (N = 9, R = 0.9999)$$

$$x_{\text{DBE}} = 0.6 \quad \tau_r = (20.3 \pm 0.4)(\eta/T)^{1.03 \pm 0.01} \quad (N = 13, R = 0.9997)$$

$$x_{\text{DBE}} = 0.8 \quad \tau_r = (28.4 \pm 1.2)(\eta/T)^{1.10 \pm 0.01} \quad (N = 10, R = 0.9994)$$

$$x_{\text{DBE}} = 1.0 \quad \tau_r = (26.4 \pm 4.0)(\eta/T)^{1.10 \pm 0.04} \quad (N = 4, R = 0.9988)$$

It is evident from these expressions that the rotational diffusion of DMDPP is significantly slower in DBE compared to [MOIM][PF<sub>6</sub>] at a given  $\eta/T$ . The boundary condition parameter ( $C_{\text{obs}}$ ), which has been obtained from the slopes of  $\tau_r$  versus  $\eta/T$  plots, increases by a factor of 2.75 with an increase in  $x_{\text{DBE}}$  from 0 to 1. The probable reasons for the observed behavior could be due to the incidence of size effects or the organized structure of the ionic liquid. As mentioned earlier, the SED theory calculates the boundary condition parameter by considering only the size of the solute and this premise works satisfactorily as long as the size of the solvent ( $V_s$ ) is much smaller than the size of the solute. However, in the present scenario, the sizes of the solute and solvent are comparable. The  $V_s$  values that have been calculated using the Edward's increment method<sup>54</sup> for DBE and [MOIM][PF<sub>6</sub>] are 190 and 316 Å<sup>3</sup>, respectively, which suggests that the size of the solvent increases by a factor of 1.7 from the organic solvent to the ionic liquid. An increase in the solvent size, in principle, decreases the solute-solvent frictional coupling, which in turn leads to the faster rotation of DMDPP in [MOIM][PF<sub>6</sub>] compared to DBE at a given  $\eta/T$ . To find out if the observed result is due to the size effects or not, quasihydrodynamic theory of Gierer-Wirtz

(GW)<sup>57</sup> has been applied. According to the GW theory, the boundary condition parameter,  $C_{\text{GW}}$ , is a function of the ratio of the volume of the solvent to the volume of the solute and is given by the following equations:

$$C_{\text{GW}} = \sigma C_0 \quad (3)$$

$$\sigma = \frac{1}{[1 + 6(V_s/V)^{1/3}C_0]} \quad (4)$$

$$C_0 = \left[ \frac{6(V_s/V)^{1/3}}{[1 + 2(V_s/V)^{1/3}]^4} + \frac{1}{[1 + 4(V_s/V)^{1/3}]^3} \right]^{-1} \quad (5)$$

The calculated  $C_{\text{GW}}$  values for DMDPP at different mole fractions of DBE are given in the Supporting Information. It can be noticed that the  $C_{\text{GW}}$  calculated in this manner decreases by less than 20% from DBE to [MOIM][PF<sub>6</sub>], which rules out the possibility that the increase in  $C_{\text{obs}}$  with  $x_{\text{DBE}}$  is due to size effects. Thus, the significant enhancement in  $C_{\text{obs}}$  from the ionic liquid to the organic solvent can be ascribed to the organized structure of [MOIM][PF<sub>6</sub>]. As already stated in the Introduction, the segregation of nonpolar and polar domains leads to the formation of organized structure in ionic liquids, especially in case of the ones with longer alkyl chains.<sup>12</sup> DMDPP, which is located in the nonpolar domains, experiences viscosity that is lower than the bulk viscosity of the ionic liquid, and as a consequence it rotates faster in [MOIM][PF<sub>6</sub>] compared to DBE at a given  $\eta/T$ . It may be recalled that the rotational diffusion of DMDPP has been investigated in 1-butyl-3-methylimidazolium-based ionic liquids with various anions.<sup>20</sup> It has been observed that reorientation times of DMDPP scale with the viscosity of the medium as the organized structure is not pronounced in ionic liquids with short alkyl chains. In [MOIM][PF<sub>6</sub>]-DBE mixtures, at low  $x_{\text{DBE}}$ , the added DBE is solubilized in the nonpolar domains of the ionic liquid, which probably leaves the organized structure of [MOIM][PF<sub>6</sub>] unaltered. Beyond  $x_{\text{DBE}} = 0.2$ , however, the DBE molecules cannot be accommodated in the nonpolar domains of the ionic liquid, resulting in the disruption of the organized structure. As a consequence, the solvent mixture turns homogeneous at the microscopic level and the solute senses the bulk viscosity, which leads to slower rotation in [MOIM][PF<sub>6</sub>]-DBE mixtures compared to the ionic liquid at a given  $\eta/T$ . In other words, the rotation of DMDPP is governed by microviscosity in [MOIM][PF<sub>6</sub>], whereas in DBE and [MOIM][PF<sub>6</sub>]-DBE mixtures it is the bulk viscosity that dictates the rotational diffusion of the solute. This result is similar to the one obtained for the nonpolar solute 9-PA in [MOIM][BF<sub>4</sub>]-DEG mixtures.<sup>9</sup> From these two studies it is apparent that the trends in the results observed for the nonpolar 9-PA and the nondipolar DMDPP in ionic liquid-organic solvent mixtures are identical irrespective of the nature of the organic solvent employed.

Figure 7 depicts  $\tau_r$  versus  $\eta/T$  plots for DPP, and it is evident from the figure that the reorientation times are closer to stick hydrodynamics. Even though DMDPP and DPP are similar in shape and size, their rotational diffusion is quite different owing to the strong hydrogen bond donating character of the latter. A close scrutiny of the tables presented in the Supporting Information reveals that the  $\tau_r$  values of DPP are a factor of 2 longer than the ones obtained for DMDPP due to specific interactions with the medium. Besides these differences, another important feature that can be noticed from Figure 7 is that there is no gradual variation in the reorientation times of DPP with an

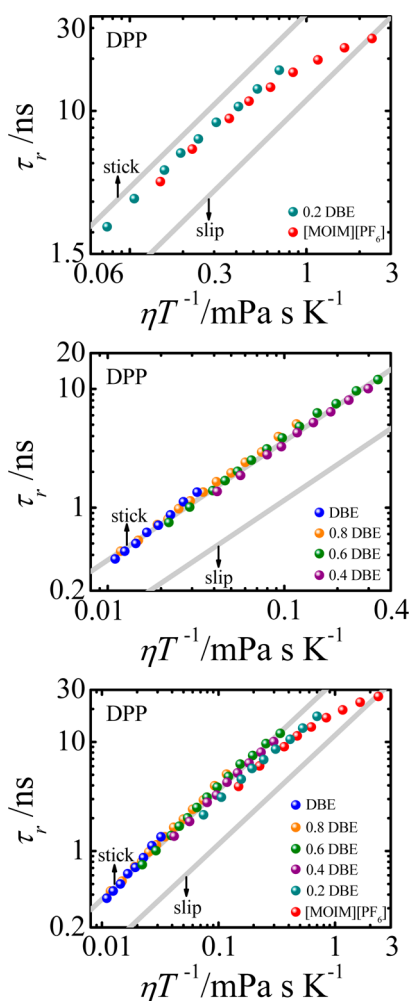


**Figure 7.** Plots of  $\tau_r$  vs  $\eta/T$  for DPP in [MOIM][PF<sub>6</sub>]-DBE mixtures. The top panel displays the data for  $x_{\text{DBE}} = 0.0$ – $0.2$ , the middle panel for  $x_{\text{DBE}} = 0.4$ – $1.0$ , and the entire data is shown in the bottom panel. The SED slip and stick lines are also shown in all the panels.

increase in  $x_{\text{DBE}}$ . Instead, two sets of reorientation times have been obtained, one corresponding to neat ionic liquid and  $x_{\text{DBE}} = 0.2$ , and the other  $x_{\text{DBE}} = 0.4$ – $1.0$ . The two sets of data are presented in the top and middle panels of Figure 7, while the bottom panel displays the entire data. Linear least-squares fits of the data give the following relationships between  $\tau_r$  and  $\eta/T$ :

$$x_{\text{DBE}} = 0.0\text{--}0.2 \quad \tau_r = (22.0 \pm 0.8)(\eta/T)^{0.87 \pm 0.02} \quad (N = 15, R = 0.9949)$$

$$x_{\text{DBE}} = 0.4\text{--}1.0 \quad \tau_r = (38.0 \pm 1.4)(\eta/T)^{1.01 \pm 0.01} \quad (N = 43, R = 0.9972)$$

It has been well-established that DPP forms various types of aggregates in the solid state as a consequence of intermolecular hydrogen bonding.<sup>58,59</sup> Due to this reason, it is soluble only in hydrogen bond accepting solvents. It can be noticed that, for a given  $\eta/T$ , the reorientation times of DPP are longer in DBE compared to [MOIM][PF<sub>6</sub>], which suggests that the solute experiences stronger hydrogen bonding interactions with the organic solvent. DPP dissolves in [MOIM][PF<sub>6</sub>] and DBE by forming hydrogen bonds with the anion and the oxygen atom of the ether group, respectively. However, at ambient temperatures, the hydrogen bonding interactions between DPP and [PF<sub>6</sub>] are weaker as the anion is not readily accessible to the solute because of the organized structure of the ionic liquid. Upon increasing the temperature, the aggregated nonpolar

domains of the ionic liquid diffuse and smear out.<sup>60</sup> As a result, accessibility of the anions to the solute increases, which leads to stronger hydrogen-bonding interactions between DPP and [PF<sub>6</sub>]. In fact, this effect can be readily noticed in Figure 7, where significant deviations from linearity have been observed in the  $\tau_r$  versus  $\eta/T$  plot for DPP in [MOIM][PF<sub>6</sub>] at ambient temperatures (298–308 K). Because of this reason, the three points are not included in the least-squares fit of the data involving neat ionic liquid and  $x_{\text{DBE}} = 0.2$ . It may be noted that a similar nonlinear behavior has been observed for DMDPP at ambient temperatures in [MOIM][PF<sub>6</sub>]. However, the reorientation times of DMDPP are in the subslip regime, whereas those of DPP are in between slip and stick limits (see Figures 6 and 7). Thus, the pronounced nonlinear patterns observed in the  $\tau_r$  versus  $\eta/T$  plots for DMDPP and DPP at ambient temperatures in [MOIM][PF<sub>6</sub>] arise due to vastly different reasons. At  $x_{\text{DBE}} = 0.2$ , the added DBE molecules are solubilized in the nonpolar domains of the ionic liquid due to their nondipolar nature. Since DPP is not soluble in alkane-like environment, it is located in the neighborhood of [PF<sub>6</sub>] anions. Therefore, the rotation of DPP at low concentrations of DBE ( $x_{\text{DBE}} = 0.2$ ) is similar to that observed in [MOIM][PF<sub>6</sub>]. From  $x_{\text{DBE}} = 0.4$ – $1.0$ , however, there is no variation in the rotational diffusion of DPP, as the organized structure of [MOIM][PF<sub>6</sub>] gets disrupted and the solute experiences specific interactions with DBE rather than the anion of the ionic liquid.

#### 4. CONCLUSIONS

From the fluorescence anisotropy measurements carried out with the nondipolar solutes DMDPP and DPP in [MOIM]-[PF<sub>6</sub>]-DBE mixtures the following conclusions can be drawn. Addition of DBE alters the rotational diffusion of both DMDPP and DPP, albeit in a contrasting manner. For a given  $\eta/T$ , the reorientation times of DMDPP become progressively slower with an increase in  $x_{\text{DBE}}$ . On the other hand, two sets of reorientation times have been obtained for DPP, corresponding to  $x_{\text{DBE}} = 0.0$ – $0.2$  and  $x_{\text{DBE}} = 0.4$ – $1.0$ . Addition of the organic solvent gradually disrupts the organized structure of the ionic liquid and turns the solvent mixture homogeneous at the microscopic level, which is evident from the trends observed in the rotational diffusion of DMDPP. The hydrogen bond donating solute, in contrast, experiences specific interactions with [PF<sub>6</sub>] anion in neat ionic liquid and at  $x_{\text{DBE}} = 0.2$ . However, from  $x_{\text{DBE}} = 0.4$ – $1.0$ , hydrogen bonding with the organic solvent takes precedence. Thus, despite their similarity in size and shape, the influence of a low viscous nondipolar organic solvent on the rotational diffusion of DMDPP and DPP in [MOIM][PF<sub>6</sub>] is vastly different owing to the nature of the interactions they experience with the medium.

#### ■ ASSOCIATED CONTENT

##### Supporting Information

Reorientation times of DMDPP and DPP in [MOIM][PF<sub>6</sub>]-DBE mixtures and their viscosities as a function of temperature,  $V_s$  and  $C_{\text{GW}}$  values of DMDPP at different mole fractions of DBE. This material is available free of charge via the Internet at <http://pubs.acs.org>.

#### ■ AUTHOR INFORMATION

##### Corresponding Author

\*E-mail: [gbdutt@barc.gov.in](mailto:gbdutt@barc.gov.in).

## Notes

The authors declare no competing financial interest.

## ACKNOWLEDGMENTS

Financial assistance provided by the Department of Atomic Energy for the project no. 2008/38/04-BRNS is acknowledged. Sugosh Prabhu is grateful to the University Grants Commission for the award of Senior Research Fellowship.

## REFERENCES

- (1) Paul, A.; Samanta, A. Effect of Nonpolar Solvents on the Solute Rotation and Solvation Dynamics in an Imidazolium Ionic Liquid. *J. Phys. Chem. B* **2008**, *112*, 947–953.
- (2) Makowska, A.; Dyoniziak, E.; Siporska, A.; Szydłowski, J. Miscibility of Ionic Liquids with Polyhydric Alcohols. *J. Phys. Chem. B* **2010**, *114*, 2504–2508.
- (3) Trivedi, S.; Pandey, S. Interactions within a [Ionic Liquid + Poly(ethylene glycol)] Mixture Revealed by Temperature-Dependent Synergistic Dynamic Viscosity and Probe-Reported Microviscosity. *J. Phys. Chem. B* **2011**, *115*, 7405–7416.
- (4) Li, B.; Wang, Y.; Wang, X.; Vdovic, S.; Guo, Q.; Xia, A. Spectroscopic Evidence for Unusual Microviscosity in Imidazolium Ionic Liquid and Tetraethylene Glycol Dimethyl Ether Cosolvent Mixtures. *J. Phys. Chem. B* **2012**, *116*, 13272–13281.
- (5) Lawler, C.; Fayer, M. D. The Influence of Lithium Cations on Dynamics and Structure of Room Temperature Ionic Liquids. *J. Phys. Chem. B* **2013**, *117*, 9768–9774.
- (6) Zhang, X.-X.; Liang, M.; Hunger, J.; Buchner, R.; Maroncelli, M. Dielectric Relaxation and Solvation Dynamics in a Prototypical Ionic Liquid + Dipolar Protic Liquid Mixture: 1-Butyl-3-Methylimidazolium Tetrafluoroborate + Water. *J. Phys. Chem. B* **2013**, *117*, 15356–15368.
- (7) Liang, M.; Zhang, X.-X.; Kaintz, A.; Ernsting, N. P.; Maroncelli, M. Solvation Dynamics in a Prototypical Ionic Liquid + Dipolar Aprotic Liquid Mixture: 1-Butyl-3-methylimidazolium Tetrafluoroborate + Acetonitrile. *J. Phys. Chem. B* **2014**, *118*, 1340–1352.
- (8) Prabhu, S. R.; Dutt, G. B. Rotational Diffusion of Nonpolar and Charged Solutes in Propylammonium Nitrate–Propylene Glycol Mixtures: Does the Organized Structure of the Ionic Liquid Influence Solute Rotation? *J. Phys. Chem. B* **2014**, *118*, 2738–2745.
- (9) Prabhu, S. R.; Dutt, G. B. Rotational Diffusion of Organic Solutes in 1-Methyl-3-octylimidazolium Tetrafluoroborate–Diethylene Glycol Mixtures: Influence of Organic Solvent on the Organized Structure of the Ionic Liquid. *J. Phys. Chem. B* **2014**, *118*, 5562–5569.
- (10) Jiang, H. J.; FitzGerald, P. A.; Dolan, A.; Atkin, R.; Warr, G. G. Amphiphilic Self-Assembly of Alkanols in Protic Ionic Liquids. *J. Phys. Chem. B* **2014**, *118*, 9983–9990.
- (11) Barra, K. M.; Sabatini, R. P.; Zachery, P.; McAtee, Z. P.; Heitz, M. P. Solvation and Rotation Dynamics in the Trihexyl(tetradecyl)-phosphonium Chloride Ionic Liquid/Methanol Cosolvent System. *J. Phys. Chem. B* **2014**, *118*, 12979–12992.
- (12) Chen, S.; Zhang, S.; Liu, X.; Wang, J.; Wang, J.; Dong, K.; Sun, J.; Xu, B. Ionic Liquid Clusters: Structure, Formation Mechanism, and Effect on the Behavior of Ionic Liquids. *Phys. Chem. Chem. Phys.* **2014**, *16*, 5893–5906.
- (13) Ingram, J. A.; Moog, R. S.; Ito, N.; Biswas, R.; Maroncelli, M. Solute Rotation and Solvation Dynamics in a Room-Temperature Ionic Liquid. *J. Phys. Chem. B* **2003**, *107*, 5926–5932.
- (14) Ito, N.; Arzhantsev, S.; Heitz, M.; Maroncelli, M. Solvation Dynamics and Rotation of Coumarin 153 in Alkylphosphonium Ionic Liquids. *J. Phys. Chem. B* **2004**, *108*, 5771–5777.
- (15) Jin, H.; Baker, G. A.; Arzhantsev, S.; Dong, J.; Maroncelli, M. Solvation and Rotational Dynamics of Coumarin 153 in Ionic Liquids: Comparisons to Conventional Solvents. *J. Phys. Chem. B* **2007**, *111*, 7291–7302.
- (16) Mali, K. S.; Dutt, G. B.; Mukherjee, T. Do Organic Solutes Experience Specific Interactions with Ionic Liquids? *J. Chem. Phys.* **2005**, *123*, 174504/1–174504/7.
- (17) Gangamallaiiah, V.; Dutt, G. B. Influence of the Organized Structure of 1-Alkyl-3-methylimidazolium Tetrafluoroborates on the Rotational Diffusion of Structurally Similar Nondipolar Solutes. *J. Phys. Chem. B* **2014**, *118*, 13711–13717.
- (18) Dutt, G. B. Influence of Specific Interactions on the Rotational Dynamics of Charged and Neutral Solutes in Ionic Liquids Containing Tris(pentafluoroethyl)trifluorophosphate (FAP) Anion. *J. Phys. Chem. B* **2010**, *114*, 8971–8977.
- (19) Karve, L.; Dutt, G. B. Rotational Diffusion of Neutral and Charged Solutes in Ionic Liquids: Is Solute Reorientation Influenced by Nature of Cation? *J. Phys. Chem. B* **2011**, *115*, 725–729.
- (20) Karve, L.; Dutt, G. B. Rotational Diffusion of Neutral and Charged Solutes in 1-Butyl-3-Methylimidazolium Based Ionic Liquids: Influence of Nature of Anion on Solute Rotation. *J. Phys. Chem. B* **2012**, *116*, 1824–1830.
- (21) Karve, L.; Dutt, G. B. Role of Specific Interactions on the Rotational Diffusion of Organic Solutes in a Protic Ionic Liquid–Propylammonium Nitrate. *J. Phys. Chem. B* **2012**, *116*, 9107–9113.
- (22) Gangamallaiiah, V.; Dutt, G. B. Rotational Diffusion of Nonpolar and Ionic Solutes in 1-Alkyl-3-Methylimidazolium bis-(trifluoromethylsulfonyl)imides: Is Solute Rotation Always Influenced by the Length of the Alkyl Chain on the Imidazolium Cation? *J. Phys. Chem. B* **2012**, *116*, 12819–12825.
- (23) Gangamallaiiah, V.; Dutt, G. B. Fluorescence Anisotropy of a Nonpolar Solute in 1-Alkyl-3-Methylimidazolium-Based Ionic Liquids: Does the Organized Structure of the Ionic Liquid Influence Solute Rotation? *J. Phys. Chem. B* **2013**, *117*, 5050–5057.
- (24) Gangamallaiiah, V.; Dutt, G. B. Influence of the Organized Structure of 1-Alkyl-3-Methylimidazolium-Based Ionic Liquids on the Rotational Diffusion of an Ionic Solute. *J. Phys. Chem. B* **2013**, *117*, 9973–9979.
- (25) Gangamallaiiah, V.; Dutt, G. B. Effect of Alkyl Chain Length on the Rotational Diffusion of Nonpolar and Ionic Solutes in 1-Alkyl-3-Methylimidazolium bis-(trifluoromethylsulfonyl)-imides. *J. Phys. Chem. B* **2013**, *117*, 12261–12267.
- (26) Prabhu, S. R.; Dutt, G. B. Rotational Diffusion of Nondipolar and Charged Solutes in Alkyl Substituted Imidazolium Triflimides: Effect of C2 Methylation on Solute Rotation. *J. Phys. Chem. B* **2014**, *118*, 9420–9426.
- (27) Fruchey, K.; Fayer, M. D. Dynamics in Organic Ionic Liquids in Distinct Regions Using Charged and Uncharged Orientational Relaxation Probes. *J. Phys. Chem. B* **2010**, *114*, 2840–2845.
- (28) Khara, D. C.; Samanta, A. Rotational Dynamics of Positively and Negatively Charged Solutes in Ionic Liquid and Viscous Molecular Solvent Studied by Time-Resolved Fluorescence Anisotropy Measurements. *Phys. Chem. Chem. Phys.* **2010**, *12*, 7671–7677.
- (29) Khara, D. C.; Samanta, A. Fluorescence Response of Coumarin-153 in N-Alkyl-N-methylmorpholinium Ionic Liquids: Are These Media More Structured than the Imidazolium Ionic Liquids? *J. Phys. Chem. B* **2012**, *116*, 13430–13438.
- (30) Khara, D. C.; Kumar, J. P.; Mondal, N.; Samanta, A. Effect of the Alkyl Chain Length on the Rotational Dynamics of Nonpolar and Dipolar Solutes in a Series of N-Alkyl-N-Methylmorpholinium Ionic Liquids. *J. Phys. Chem. B* **2013**, *117*, 5156–5164.
- (31) Das, S. K.; Sarkar, M. Solvation and Rotational Relaxation of Coumarin 153 and 4-Aminophthalimide in a New Hydrophobic Ionic Liquid: Role of N–H...F Interaction on Solvation Dynamics. *Chem. Phys. Lett.* **2011**, *515*, 23–28.
- (32) Das, S. K.; Sarkar, M. Solvation and Rotational Relaxation of Coumarin 153 in a New Hydrophobic Ionic Liquid: An Excitation Wavelength Dependence Study. *J. Lumin.* **2012**, *132*, 368–374.
- (33) Das, S. K.; Sarkar, M. Rotational Dynamics of Coumarin-153 and 4-Aminophthalimide in 1-Ethyl-3-methylimidazolium Alkylsulfate Ionic Liquids: Effect of Alkyl Chain Length on the Rotational Dynamics. *J. Phys. Chem. B* **2012**, *116*, 194–202.
- (34) Das, S. K.; Sahu, P. K.; Sarkar, M. Diffusion–Viscosity Decoupling in Solute Rotation and Solvent Relaxation of Coumarin 153 in Ionic Liquids Containing Fluoroalkylphosphate (FAP) Anion: A



Thermophysical and Photophysical Study. *J. Phys. Chem. B* **2013**, *117*, 636–647.

(35) Sahu, P. K.; Das, S. K.; Sarkar, M. Toward Understanding Solute–Solvent Interaction in Room-Temperature Mono- and Dicationic Ionic Liquids: A Combined Fluorescence Spectroscopy and Mass Spectrometry Analysis. *J. Phys. Chem. B* **2014**, *118*, 1907–1915.

(36) Guo, J.; Han, K. S.; Mahurin, S. M.; Baker, G. A.; Hillesheim, P. C.; Dai, S.; Hagaman, E. W.; Shaw, R. W. Rotational and Translational Dynamics of Rhodamine 6G in a Pyrrolidinium Ionic Liquid: A Combined Time-Resolved Fluorescence Anisotropy Decay and NMR Study. *J. Phys. Chem. B* **2012**, *116*, 7883–7890.

(37) Guo, J.; Mahurin, S. M.; Baker, G. A.; Hillesheim, P. C.; Dai, S.; Shaw, R. W. Influence of Solute Charge and Pyrrolidinium Ionic Liquid Alkyl Chain Length on Probe Rotational Reorientation Dynamics. *J. Phys. Chem. B* **2014**, *118*, 1088–1096.

(38) Dutt, G. B.; Srivatsavoy, V. J. P.; Sapre, A. V. Rotational Dynamics of Pyrrolopyrrole Derivatives in Alcohols: Does Solute–Solvent Hydrogen Bonding Really Hinder Molecular Rotation? *J. Chem. Phys.* **1999**, *110*, 9623–9629.

(39) Dutt, G. B.; Srivatsavoy, V. J. P.; Sapre, A. V. Rotational Dynamics of Pyrrolopyrrole Derivatives in Glycerol: A Comparative Study with Alcohols. *J. Chem. Phys.* **1999**, *111*, 9705–9710.

(40) Dutt, G. B.; Krishna, G. R. Temperature-Dependent Rotational Relaxation of Nonpolar Probes in Mono and Diols: Size Effects versus Hydrogen Bonding. *J. Chem. Phys.* **2000**, *112*, 4676–4682.

(41) Dutt, G. B. Rotational Dynamics of Nondipolar Probes in Alkane–Alkanol Mixtures: Microscopic Friction on Hydrogen Bonding and Nonhydrogen Bonding Solute Molecules. *J. Chem. Phys.* **2000**, *113*, 11154–11158.

(42) Dutt, G. B.; Ghanty, T. K. Rotational Dynamics of Nondipolar Probes in Electrolyte Solutions: Can Specific Interactions be Modeled as Dielectric Friction? *J. Chem. Phys.* **2002**, *116*, 6687–6693.

(43) Dutt, G. B.; Ghanty, T. K. Rotational Dynamics of Nondipolar Probes in Associative Solvents: Modeling of Hydrogen Bonding Interactions using the Extended Charge Distribution Theory of Dielectric Friction. *J. Chem. Phys.* **2003**, *118*, 4127–4133.

(44) Dutt, G. B.; Ghanty, T. K. Rotational Dynamics of Nondipolar Probes in Ethanol: How Does the Strength of the Solute–Solvent Hydrogen Bond Impede Molecular Rotation? *J. Chem. Phys.* **2003**, *119*, 4768–4774.

(45) Dutt, G. B.; Ghanty, T. K. Rotational Dynamics of Nondipolar Probes in Butanols: Correlation of Reorientation Times with Solute–Solvent Interaction Strengths. *J. Phys. Chem. A* **2004**, *108*, 6090–6095.

(46) Dutt, G. B. Molecular Rotation as a Tool for Exploring Specific Solute–Solvent Interactions. *ChemPhysChem* **2005**, *6*, 413–418.

(47) Tian, Y.; Wang, X.; Wang, J. Densities and Viscosities of 1-Butyl-3-methylimidazolium Tetrafluoroborate + Molecular Solvent Binary Mixtures. *J. Chem. Eng. Data* **2008**, *53*, 2056–2059.

(48) Mokhtarani, B.; Sharifi, A.; Mortaheb, H. R.; Mirzaei, M.; Mafi, M.; Sadeghian, F. Density and Viscosity of 1-Butyl-3-methylimidazolium Nitrate with Ethanol, 1-Propanol, or 1-Butanol at Several Temperatures. *J. Chem. Thermodyn.* **2009**, *41*, 1432–1438.

(49) Mokhtarani, B.; Sharifi, A.; Mortaheb, H. R.; Mirzaei, M.; Mafi, M.; Sadeghian, F. Densities and Viscosities of Pure 1-Methyl-3-octylimidazolium Nitrate and Its Binary Mixtures with Alcohols at Several Temperatures. *J. Chem. Eng. Data* **2010**, *55*, 3901–3908.

(50) Mokhtarani, B.; Sharifi, A.; Mortaheb, H. R.; Mirzaei, M.; Mafi, M.; Sadeghian, F. Density and Viscosity of Pyridinium-Based Ionic Liquids and their Binary Mixtures with Water at Several Temperatures. *J. Chem. Thermodyn.* **2009**, *41*, 323–329.

(51) Anouti, M.; Vigeant, A.; Jacquemin, J.; Brigouleix, C.; Lemordant, D. Volumetric Properties, Viscosity and Refractive Index of the Protic Ionic Liquid, Pyrrolidinium Octanoate, in Molecular Solvents. *J. Chem. Thermodyn.* **2010**, *42*, 834–845.

(52) Fleming, G. R. *Chemical Applications of Ultrafast Spectroscopy*; Oxford University Press: New York, 1986.

(53) Waldeck, D. H. The Role of Solute–Solvent Friction in Large-Amplitude Motions. In *Conformational Analysis of Molecules in the*

*Excited States*; Waluk, J., Ed.; Wiley-VCH: New York, 2000; pp 113–176.

(54) Edward, J. T. Molecular Volumes and the Stokes–Einstein Equation. *J. Chem. Educ.* **1970**, *47*, 261–270.

(55) Perrin, F. Mouvement Brownien d'un Ellipsoïde—I. Dispersion Diélectrique pour des Molécules Ellipsoïdales. *J. Phys. Radium* **1934**, *5*, 497–511.

(56) Hu, C. M.; Zwanzig, R. Rotational Friction Coefficients for Spheroids with the Slipping Boundary Condition. *J. Chem. Phys.* **1974**, *60*, 4354–4357.

(57) Gierer, A.; Wirtz, K. Molekulare Theorie der Mikrorreibung. *Z. Naturforsch., A: Phys. Sci.* **1953**, *8*, 532–538.

(58) Adachi, M.; Nakamura, S. Absorption Spectrum Shift in the Solid State. A MO Study of Pyrrolopyrrole Pigment. *J. Phys. Chem.* **1994**, *98*, 1796–1801.

(59) Srivatsavoy, V. J. P.; Moser, J.-E.; Grätzel, M.; Chassot, L. Surface Modification of a Hydrogen-Bonded Pigment: A Fluorescence Spectroscopy Study. *J. Colloid Interface Sci.* **1999**, *216*, 189–192.

(60) Wang, Y.; Voth, G. A. Tail Aggregation and Domain Diffusion in Ionic Liquids. *J. Phys. Chem. B* **2006**, *110*, 18601–18608.